PHILOSOPHICAL TRANSACTIONS OF THE ROYAL SOCIETY A MATHEMATICAL, PHYSICAL & ENGINEERING SCIENCES

Silo pressure predictions using discrete–element and finite–element analyses

J. M. Rotter, J. M.F. G. Holst, J. Y. Ooi and A. M. Sanad

Phil. Trans. R. Soc. Lond. A 1998 **356**, 2685-2712
doi: 10.1098/rsta.1998.0293

THE ROYAL SOCIETY

Silo pressure predictions using discrete-element and finite-element analyses

By J. M. Rotter, J. M. F. G. Holst, J. Y. Ooi and A. M. Sanad†

Department of Civil and Environmental Engineering, University of Edinburgh, King's Buildings, West Mains Road, Edinburgh EH9 3JN, UK

The storage of granular solids in silos provides many interesting problems concerning pressures and flow. It is difficult to obtain repeatable and trustworthy results from either experimental studies or theoretical modelling. Comparisons of the best computational models with experiments are, at best, weak, and provide little assurance of the accuracy of any existing predictive model. The study described here was undertaken to explore the predictions of different models on a set of simplified exercise silo problems. For these problems, no experimental results exist, but simpler tests for truth can be used.

This paper reports briefly on an international collaborative study into the predictive capacity of current discrete-element and finite-element calculations for the behaviour of granular solids in silos. The predictions of one research group, however eminent, are often not regarded as authoritative by others, so a commonly agreed theoretical solution of simple silo exercises, using different computational models from research groups around the world, is a valuable goal. Further, by setting the same unbiased exercise for both finite elements and discrete elements, a better understanding was sought of the relationships between the two methods and of the strengths of each method in practical silo modelling.

The key findings are outlined here from three of the challenge problems: filling a silo; discharge of granular solid from a flat-bottomed silo; and discharge from a silo with a tapered hopper. Both computational methods display considerable shortcomings for these difficult exercises. Different research groups make widely different predictions, even when the problem statement is very detailed. There is much scope for further comparative studies to identify the reasons why different models based on comparable assumptions can produce such varied predictions.

Keywords: discharge from a silo; filling of a silo; granular solid; challenge calculations; numerical analyses; wall pressures

1. Introduction

Silos are used to store a very wide range of granular solids in many different industries. Current design is based almost exclusively on simplified interpretations of experimental observations in the light of very simple theories. It is widely recognized (Rotter *et al*. 1986; Nielsen, this issue), however, that it is very difficult to obtain reliable information from these experiments, and that many experiments have been grossly misinterpreted in the past. Over the last two decades, a major effort in many

† All the collaborators should properly be described as co-authors, but their number precludes this here.

countries has been put into developing computational models for the behaviour of granular solids in silos (see, for example, Bishara *et al*. 1977, 1981; Jofriet *et al*. 1977; Mahmoud & Abdel-Sayed 1981; Smith & Lohnes 1982; Eibl *et al*. 1982; Eibl & Rombach 1988; Häußler & Eibl 1984; Runesson & Nilsson 1986; Askari & Elwi 1988; Ooi & Rotter 1989, 1990; Schmidt & Wu 1989; Wu & Schmidt 1992; Aribert & Ragneau 1990; Tejchman & Gudehus 1993; Ragneau *et al*. 1994; Yagi *et al*. 1995; Wieckowski & Klisinski 1995; Karlsson *et al*. 1998). These models, however, have been subjected to very little comparison with true silo experiments. Indeed, many of the phenomena reported from the experiments relate to solids' behaviour that cannot yet be captured by existing computational models (e.g. anisotropy arising from grain shape).

Some observers have declared that continuum modelling should be abandoned in favour of discrete-element models, but the latter have generally only been applied to silos as qualitative and illustrative demonstration calculations in the past (e.g. Thornton 1991; Savage 1992; Ting *et al*. 1993; Sakaguchi *et al*. 1996; Langston *et al*. 1994, 1995; Kafui & Thornton 1995). For this reason, much progress is needed in computational-model development before their predictions can be used with confidence for design calculations. Reliable computational models are needed if the design process is to be changed from being an art into becoming a science.

Two main types of computational model are widely used to predict the responses of granular solids in silos: continuum models (mostly based on finite elements, FEM); and discrete models (here termed the discrete-element method, DEM).

An international collaborative study was conducted to explore the power of discrete-element and finite-element calculations to predict granular-solid behaviour in silos. The study was undertaken to explore the predictions of different computational models on simplified exercise problems, for which no precise experimental results exist, but for which simpler tests for truth might be used, such as the order of magnitude and form of the prediction compared with empirically derived design rules. The latter represent an integration of knowledge from a large database of test results.

The collaboration sought to establish the extent to which computational models with different attributes—and used by well-known research groups around the world—could produce a common prediction of a set of simple theoretical exercise problems associated with silos. In addition, it was hoped that the exercise conducted using both finite-element and discrete-element modelling on the same problem in an unbiased manner, would lead to a better understanding of the relationships between the two methods, and might identify the strengths of each method for use in practical modelling. The goal of engineering research in silos is the functionally effective and structurally safe design of silos, so the potential of the calculations to be practically relevant was an important measure of success.

This paper reports some of the key findings from three exercise problems: filling a silo; the discharge of a granular solid from a flat-bottomed silo; and discharge from a silo with a tapered hopper. The results show that both computational methods have considerable shortcomings for these challenging problems and that the predictions from different groups vary widely, even when the exercises are very precisely defined. There is, evidently, much scope for further comparative studies to identify the reasons why different models based on similar assumptions can produce such varied predictions.

PHILOSOPHICAL TRANSACTIONS OF THE ROYAL SOCIETY A MATHEMATICAL, PHYSICAL & ENGINEERING SCIENCES

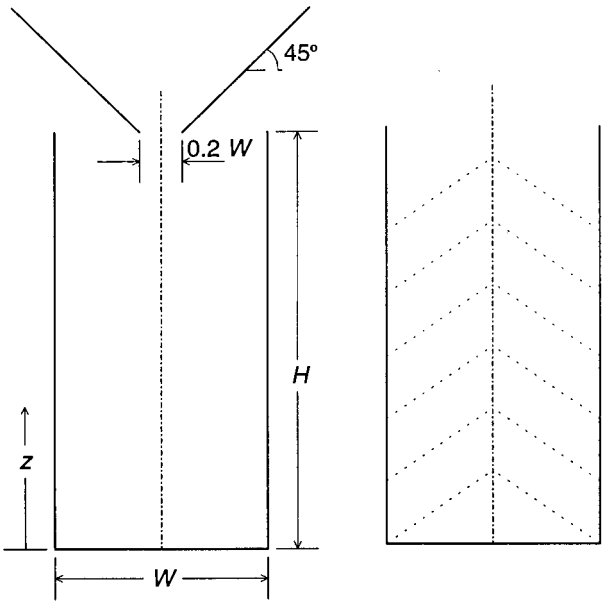

Figure 1. Geometry of silo for exercise 1.

2. Standard-exercise descriptions

The three standard exercises described here involve the central filling (figure 1) and central discharge of a parallel-sided silo with either a flat bottom or a steep-hopper bottom (figure 2). The study was restricted to a two-dimensional planar flow analysis (plane strain for FEM, circular rods for DEM) to enable as many research groups as possible to participate in the project.

A precise definition of the filling process is important, as it determines the packing structure and surface profile of the solid, which later influence stress and flow patterns. The properties of the particles, the pattern of fall, and the energy with which particles strike the surface are all important. The filling process for the silos was therefore defined as central-chute filling (figure 1). The DEM analysts were asked to allow the particles to fall freely from a hopper with a slot width of 1.5 m, centrally located above the test silo. For the FEM analyses, the filling process cannot be modelled and incremental progressive filling at the angle of repose was suggested.

(*a*) *Filling a silo*

For exercise 1, filling a silo, two sub-problems were defined to explore the capacity of the theoretical models to identify absolute scale effects. Two rectangular flat-bottomed silos were defined with dimensional similarity, but at different scales: one was $W = 0.5$ m, $H = 2.5$ m; the other $W = 5$ m, $H = 25$ m (figure 1).

(*b*) *Discharge of silos*

Exercise 2 concerned a flat-bottomed silo (figure 2*a*) with dimensions $W = 5$ m and $H = 25$ m, while exercise 3 had a hopper (figure 2*b*) extending over the bottom

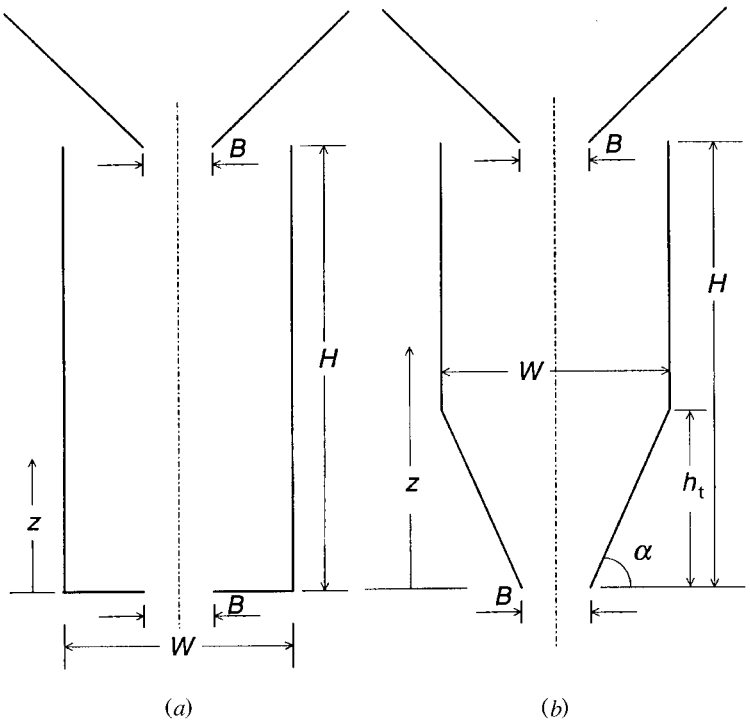

Figure 2. Geometry of silo for discharge problems.

$h_t = 8$ m with $W = 5$ m and $H = 25$ m. The first of these produces internal funnel flow, whereas the second is expected to produce mass flow of the granular solid. Thus the results should cover two different flow patterns and provide some interesting comparisons. A realistic silo geometry was chosen because scale effects are known to be important, especially in silo flow. The outlet dimension, B, for both, was chosen to be $B = 1$ m.

The limitation on the total number of particles that can be handled by most DEM analysts meant that rather large particles had to be specified. Totals of 10 000 and 8495 particles were chosen for the flat-bottom and hopper-bottom silos, respectively. The corresponding total solid volumes in the FEM analyses were 93 m^3 and 79 m^3, respectively. These numbers were chosen to give approximately the same height of fill for all analyses.

(c) *Granular-solid material definitions*

Considerable effort was made in defining the material parameters for DEM and FEM models with the aim of making meaningful comparisons between the two methods. A well-defined real sand was used for FEM. For DEM, a laboratory acrylic disc material was used in exercise 1 (Schneebeli rod assembly) because it had real measured properties, but this provided an inadequate correspondence with the FEM sand. For the discharge exercises, a fictitious DEM solid which would give a closer response to the real sand was defined, based on the results of the first exercise.

For the FEM models, loose Sacramento River sand was chosen and the material parameters extracted by Lade (1977) from his tests were adopted (table 1).

Table 1. *FEM parameters for loose Sacramento River sand (Lade 1977)*

parameter	value proposed
initial unstressed bulk material density at placement, ρ_u (kg m^{-3})	1417
modulus number, N (Janbu formula)	960
modulus exponent, n (Janbu formula)	0.57
atmospheric pressure, p_a (Pa)	100 000
equivalent Poisson's ratio, ν	0.30[a]
angle of wall friction, ϕ_w	18
angle of internal friction of bulk material, ϕ_i	35
angle of repose, ϕ_r	35
cohesion, c (Pa)	0
collapse modulus, C_c	0.00028
collapse exponent, C_p	0.94
yield constant, η_1	28
yield exponent, m	0.093
plastic potentials, R, S, t	1.0, 0.430, 0.00
work hardening constants, α, β	3, −0.076
work hardening constants, P, l	0.24, 1.25

[a] $\nu = 0.20$ was used for exercise 1 on filling a silo.

In this study, the plastic behaviour was defined either by Lade's proposed model (1977) or by a Mohr–Coulomb model with associated flow. Lade's original constitutive model adopted the Janbu (1963) formula for elastic behaviour. Corresponding properties for Boyce's (1980) elastic model and a porous elastic model (ABAQUS 1997) were also provided in the exercise description. Analysts using other models were encouraged to deduce their own parameters directly from Lade's tests.

For the DEM models, the first exercise used the Schneebeli rod assembly (monosized acrylic rods, see Sakaguchi & Ozaki (1993)) as defined in table 2. For the discharge calculations, the artificial DEM solid deemed equivalent to the sand of table 1 was termed 'Royal Mile notional cobbles'. The material parameters are given in table 3. The particle interaction is defined with either a linear inter-particle spring or a Hertz–Mindlin interaction law.

The exercise problem descriptions were very detailed and included the reasoning behind choices (Rotter *et al*. 1996; Rotter & Ooi 1995; Holst *et al*. 1999*a*). The models used by the different submissions, their predictions, and further information extracted from the results are documented in full reports (Holst *et al*. 1997; Sanad *et al*. 1997).

3. Filling predictions

The first challenge was to model the filling of a silo with a solid. The stress state in the solid and the pressures acting on the silo wall were to be found (DEM calculations could also provide information on the packing structure). A satisfactory modelling of this 'initial' state before emptying the silo is critically important because solids'

Table 2. *DEM parameters for Schneebeli rods*

parameter	value proposed	
	particle–particle	particle–wall
normal contact stiffness, K_n (N m^{-2})	1.0×10^6	1.5×10^6
tangential contact stiffness, K_s (N m^{-2})	1.0×10^5	1.5×10^5
coefficient of restitution, e	0.6	0.6
coefficient of friction, μ	0.43	0.33
normal damping constant, C_n (N m^{-1}·s m^{-1})	150	380
tangential damping constant, C_s (N m^{-1}·s m^{-1})	0	0
solid particles density, ρ_p (kg m^{-3})	1190	
mean particle diameter (m)	0.01 (exercise 1B: 0.1)	
particle shape	circular rod	
particle size distribution	diameters normally distributed: CoV = 5%	
number of particles	10 000	
global damping coefficient	0.0	

flow and silo discharge phenomena depend on the conditions produced during filling. Silo filling was thus chosen as the first exercise, despite its apparent simplicity.

The problem description was developed with care, circulated to potential participants and revised. The final problem description went to some 130 different groups. A total of 40 calculations were received: each submission was subjected to the same analysis.

Probably the most important prediction from the analysis is the pressure distribution acting on the silo wall. This should differ from hydrostatic distributions because the static strength of solids leads to differences between the horizontal and vertical stresses, and is strongly affected by wall friction, which progressively transfers vertical loads into the walls. Numerical predictions of wall pressures, p, can be usefully compared with those of the simple Janssen theory (1895)

$$p = \frac{\gamma W}{2\mu}(1 - \mathrm{e}^{-2\mu k((H_0 - z)/W)}), \tag{3.1}$$

where γ is the bulk density, H_0 is the mean top-surface height, z is the vertical coordinate above the silo base, and W is the width of the silo. The remaining two material parameters are the wall friction coefficient, μ, and the lateral pressure ratio, k (the ratio of normal wall pressure to the mean vertical stress in the solid), both of which may be taken as unknown and dependent on the macroscopic characterization of the solid achieved by the adopted constitutive laws of the numerical model. It is widely accepted amongst silo experimentalists that the Janssen theory provides a good first-order model to represent filling pressures.

Table 3. *DEM parameters for Royal Mile notional cobbles*

parameter	value proposed	
	particle–particle	particle–wall
normal contact stiffness, K_n (N m^{-2})	1.0×10^4	1.5×10^4
tangential contact stiffness, K_s (N m^{-2})	1.0×10^3	1.5×10^3
coefficient of restitution, e	0.3	0.3
coefficient of friction, μ	1.0	0.5
normal damping constant, C_n (N m^{-1}·s m^{-1})	8.6	10.5
tangential damping constant, C_s (N m^{-1}·s m^{-1})	0.86	1.05
solid particles density, ρ_p (kg m^{-3})	1607	
mean particle diameter (m)	0.10	
particle shape	circular rod	
particle size distribution	diameters normally distributed: CoV = 20%	
global damping coefficient	0.0	

(*a*) *Finite-element predictions*

A huge volume of valuable data was received, of which only a part has been fully evaluated. Although the exercise was very precisely defined and a well-documented real sand was chosen as the stored solid, the different programs gave surprisingly different predictions of the stresses after filling (Holst *et al*. 1999*a*). The scatter shows that the requirements for a reliable finite-element analysis of filling have not yet been adequately studied or published, and that they remain unknown at present or are known by so few that they cannot be classed as established scientific fact. It should be noted that the majority of the literature in this field is concerned with the prediction of discharge pressures, and the filling state has often been ignored as trivial. Much further research is needed on the prediction of the filling state if FEM is to be a useful, practical predictive tool.

An example prediction of silo wall pressures is shown in figure 3 (submission 2: here termed the reference calculation), with a corresponding Janssen curve. This shows that there is a good match between the FEM prediction and Janssen theory (assuming an appropriate choice of k and μ) except near the surface and close to the base. The former is caused by the Janssen assumption of a level upper boundary, so that the starting point for the curve must be higher than the true first wall contact to ensure vertical equilibrium is met (this discrepancy makes surprisingly little difference). The latter is caused by the base boundary condition, which is ignored in Janssen's theory, but causes very low pressures in the wall/base corner, above which lies a local pressure peak.

Silo bases generally behave in a rough manner, but, where a smooth base is assumed, a slightly different local pressure pattern develops with higher local values near the base. The two different base boundary conditions, using the same program

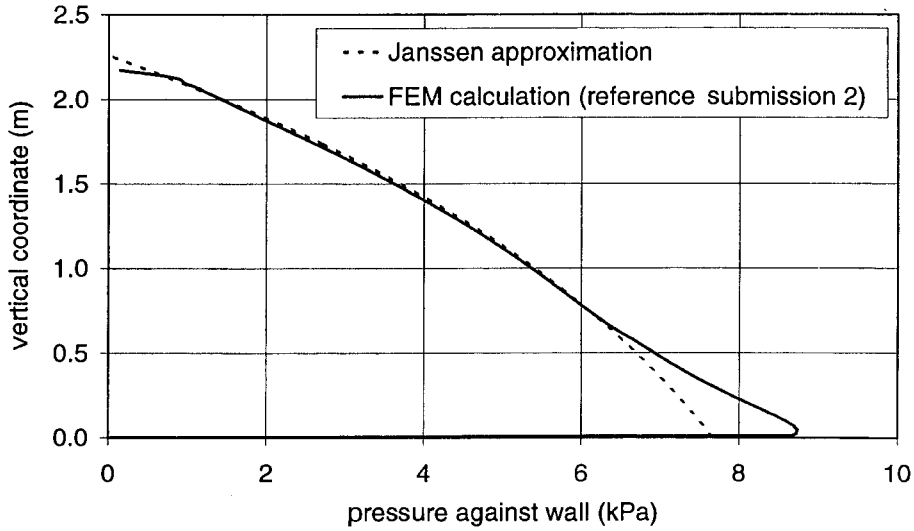

Figure 3. FEM wall pressures after filling: Janssen comparison.

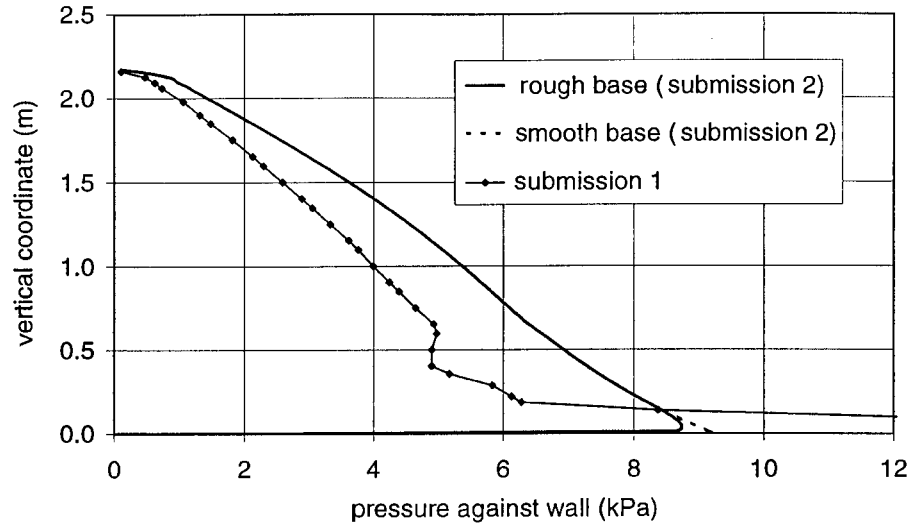

Figure 4. Effect of assumed base boundary condition in FEM.

and data file, are compared in figure 4, where the difference near the base can just be seen. The reference calculation is further compared with the prediction from submission 1, which also adopted a smooth base. It is clear that the huge pressure near the base is not only caused by a smooth base assumption, and that the level of pressures throughout the silo height is only about 75% of the reference prediction. Such differences were typical in these comparison exercises.

Of greater significance is the effect of progressive filling: the granular solid does not reach its final stressed state through a progressive increase in gravity applied to the whole solid as modelled in most calculations, but by having unstressed material placed progressively on its free surface. Several research groups claim to have investigated the consequences of modelling the progressive filling process using several

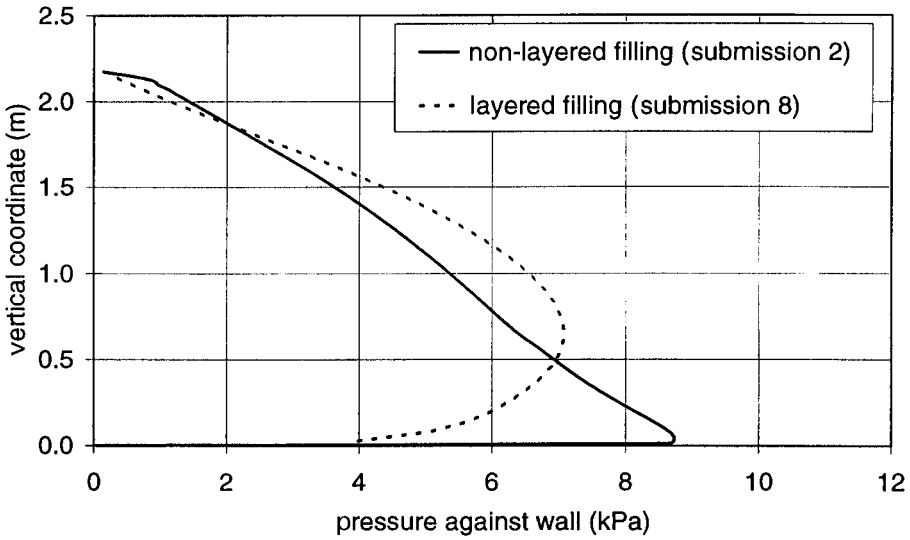

Figure 5. Effect of use of progressive filling in FEM.

layers and found it to make little difference. However, those who have adopted many extremely fine filling steps avow that major differences arise. An example is shown in figure 5, where the rounded mammary form, characteristic of progressive filling calculations (e.g. submission 8), is in marked contrast to the reference shape from simple incremented gravity. A fit to Janssen's equation is then only valid for positions high in the silo, and yields higher lateral pressure ratios, k, than a non-layered approach, for reasons which are not yet clear. This phenomenon also appears to be much more prominent under plane strain than in axisymmetry.

With these calculations as background, the full set of nine submissions from eight research groups is compared in figure 6. Two submissions adopted progressive filling in the manner described above (8 and 9), providing very similar predictions from unrelated programs on different sides of the Atlantic. Two other submissions adopted very different constitutive models (3 and 4), and rather limited material characterization, leading to curves with a superposed periodic character and rather higher pressures. The remaining five predictions all have the same form as the previously quoted reference curve and can all be approximately fitted by the Janssen equation, but notably with different values of the lateral pressure ratio k. Submissions 2, 6 and 5 are relatively close to each other.

In a finite-element calculation, the full wall friction is generally developed throughout the height of the silo because compression of the solid leads to significant slip: this contrasts with discrete-element analyses in which many particles may not be in a sliding state against the wall.

Since all participating research groups are well-respected internationally, it is clear that two key issues remain outstanding: the role of progressive filling and the lateral pressure ratio which should arise from a well-defined constitutive model for a sand. As the lateral pressure ratio plays a powerful role in silo pressures, but does not feature explicitly in the constitutive models (for good reasons), it is evident that more work is needed on this matter.

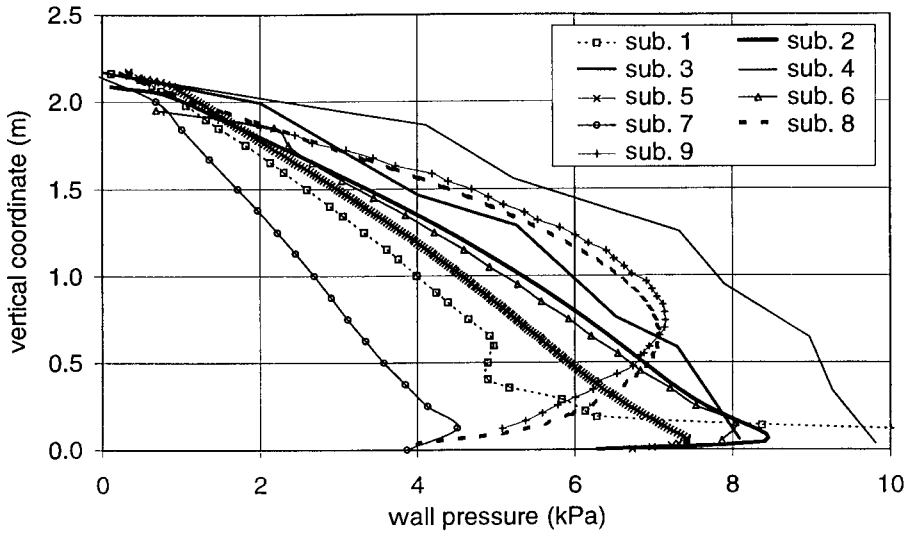

Figure 6. Comparison of FEM submissions for exercise 1.

(*b*) *Discrete-element predictions*

Essentially, the same problem was given to both continuum analysts and discrete-element analysts. A DEM analysis predicts discrete forces between the particles and the wall, so its transformation into 'pressures' which are usable for the purposes of generalization is a necessary first task. Alternative averaging schemes were used, to identify a statistically stable pressure measure: this is described in the complete report (Holst *et al*. 1997). Finally, a moving average over ten particles was adopted. The remainder of this description is based on these mean local pressures.

Many parameters were derived from the results: developed wall friction (local and macroscopic); lateral pressure ratio (local and global); bulk density; surface slope; asymmetry on opposing walls; base to wall force ratio, etc. Both the pressures and the derived parameters showed substantial scatter (Holst *et al*. 1999*b*).

A typical top-surface profile at the end of filling is shown in figure 7 (submission 10). The impact of particles has led to a central depression. Many calculations displayed an almost horizontal surface, and only one displayed a significant angle of repose: none had a repose angle comparable with the interparticle friction angle. Particle shape, rotational inertia and the coefficient of restitution all appear to affect this phenomenon.

A typical distribution of wall pressure is shown in figure 8 (submission 18). While the pressures show the general pattern of a Janssen distribution, there are substantial local departures, chiefly associated with the small number of particles making up the wall height (approximately 100). The wall shear, developed by particles in a sliding condition against the wall, is also shown: it does not follow the local pressure variations because the full particle–wall friction is not always developed, especially at pressure peaks. The incompletely developed wall friction is closely related to the use of circular particles which can easily rotate without seriously distorting the local packing arrangement.

The particle shape was explored further by one research group. The same DEM

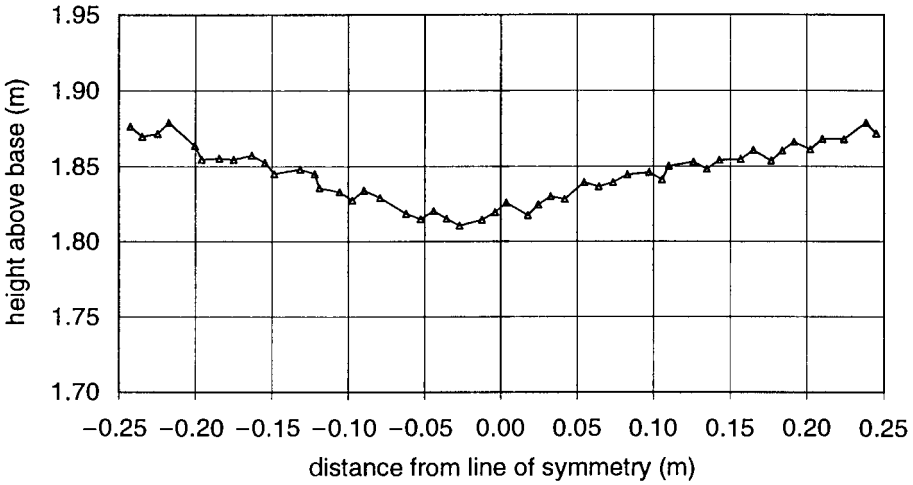

Figure 7. Top surface profile from DEM in exercise 1.

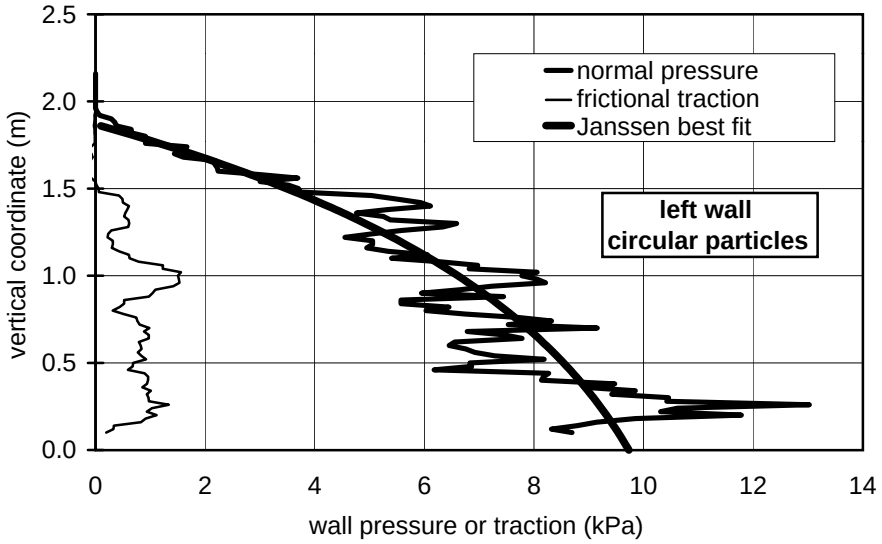

Figure 8. Typical wall-pressure distribution for DEM in exercise 1.

formulation, but using elliptical particles with an aspect ratio of 2 (submission 19), is shown in figure 9. The distribution is less scattered and much closer to a classical Janssen distribution. There is a good case for proposing that the particle shape is a critically important part of the modelling.

Although the description carefully defined the filling process so that similarity of packing should have been achieved, quite varied bulk densities were produced, with a range of 9.52–11.29 kg m^{-3}, and a good scatter between them. It appears that the particle packing structure is sensitive to the contact algorithm even in circular particle two-dimensional analyses.

The pressure distributions derived from DEM analysis were very varied and cannot be usefully portrayed on a single diagram: one of the ways of characterizing them

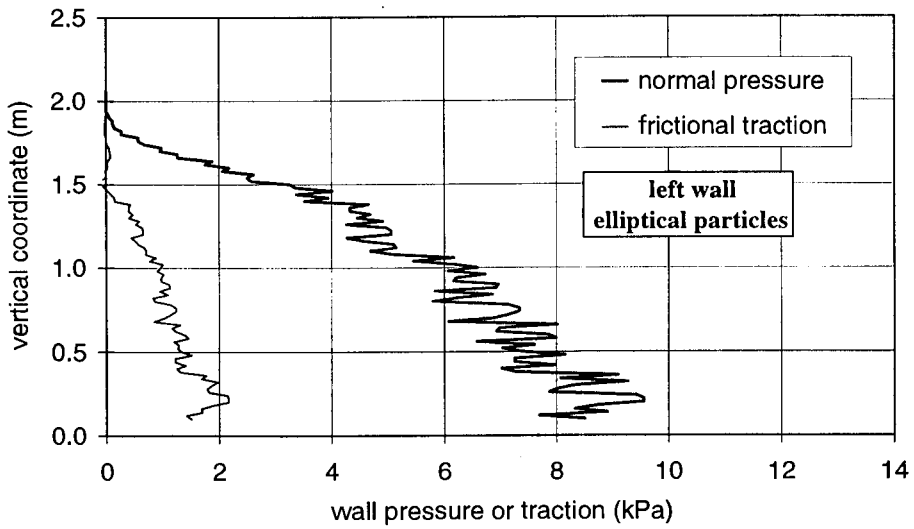

Figure 9. Pressure distribution using elliptical particles in DEM.

simply was to perform a regression analysis to find the best-fit Janssen distribution to the predicted pressures and to extract the effective values of friction, μ, and lateral pressure ratio, k. These values could then be compared from one analysis to another. The resulting extracted effective wall-friction coefficients are shown in figure 10 (reference value 0.33). The result indicates that many analyses produce very different pressure distributions, but a consensus value might be deduced lying between 0.2 and 0.3. The lateral pressure ratio is a more important parameter, about which DEM might have been expected to inform debate on granular solids. The calculated values are shown in figure 11. Almost all the values are much larger than would be expected of a real solid (0.4), this may be partly as a result of the artificial character of the Schneebeli rod assembly. These values did not correlate with other parameters, such as the predicted bulk density.

Much other information has been extracted from the DEM calculations (Holst *et al*. 1997), but space restrictions limit what can be shown here. However, many of the conclusions that one might like to draw from DEM analysis are clearly only found in some formulations and not in others. The method's lack of direct representation of a real material makes it difficult to determine which conclusions should be accepted.

(*c*) *Continuum and discrete-element comparisons*

Both the FEM and DEM submissions contained a wide range of different predictions, and no consensus solution ('right answer') could be found for either analysis. However, the reasons for differences between the FEM calculations are easier to identify and address (progressive filling and effective lateral pressure ratio). The differences between DEM submissions appear to lie within the algorithms and contact models used, and the relationship between microscopic and macroscopic parameters is only being explored now (Thornton & Anthony, this issue). Both analysis types gave pressures of the same order of magnitude and the similarities indicate that a statistical correspondence between DEM and FEM should be achievable.

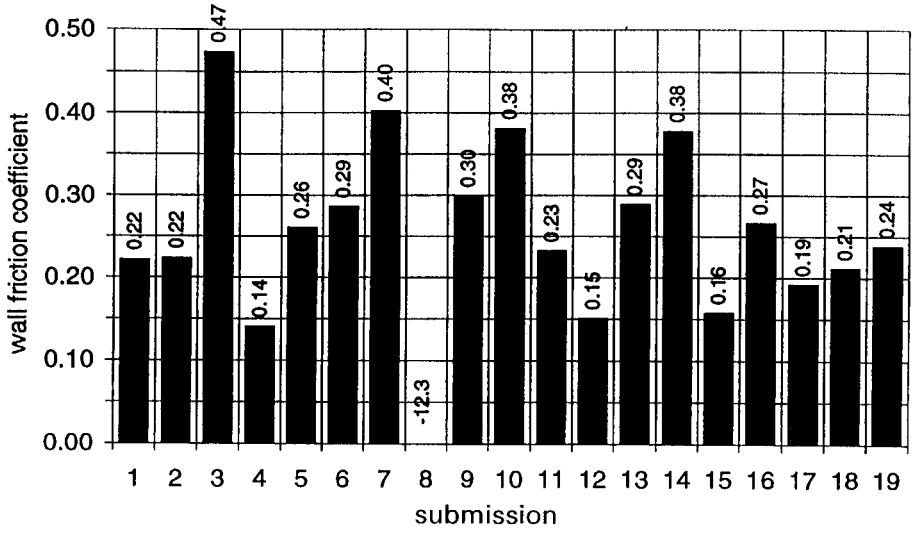

Figure 10. Inferred wall-friction coefficients for Janssen best fit to DEM.

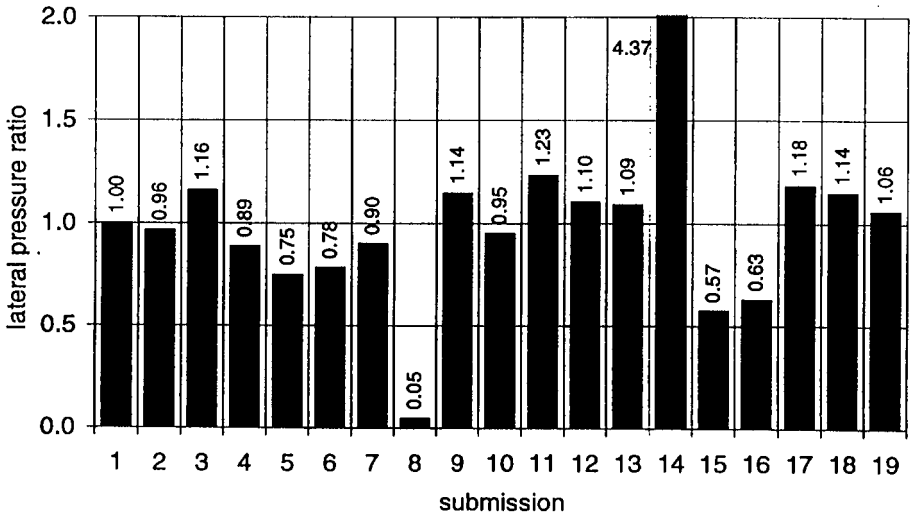

Figure 11. Inferred lateral pressure ratios for Janssen best fit to DEM.

The continuum analyses gave smoother curves for the wall pressures than the DEM calculations. It can be argued that the high scatter in DEM is a real outcome of the force-transmission systems in granular solids. While this is true, it does indicate that huge numbers of particles are needed in DEM calculations that attempt to provide meaningful predictions of complete silo phenomena, rather than assemblies of small numbers of particles (real silos typically contain between 10^7 and 10^{15} particles). Experimentalists working with pressure cells know well the size of cell needed relative to the particle size to ensure that representative mean values are observed.

The continuum analysts were generally able to reproduce the macroscopic wall-friction coefficient defined in the problem description. The DEM submissions produced a global wall-friction coefficient well below the individual particle–wall contact

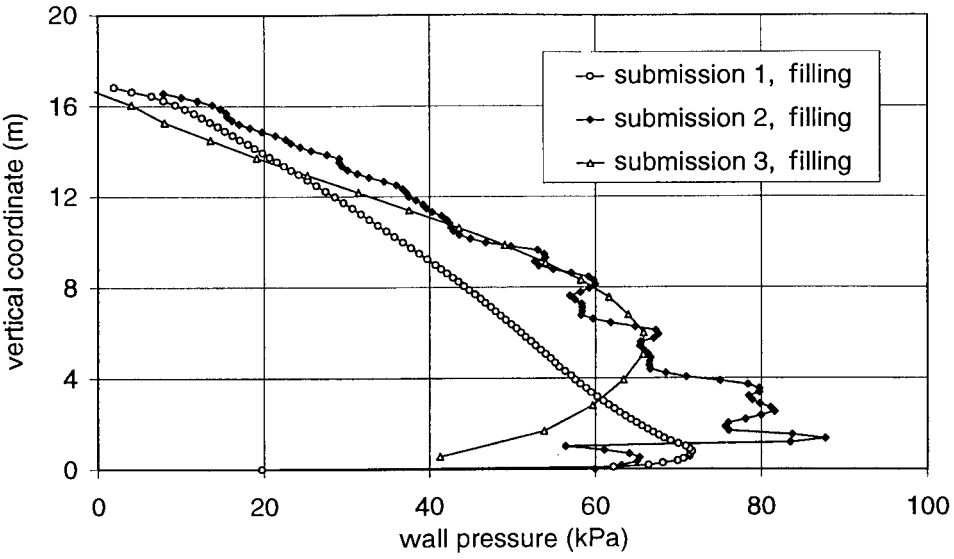

Figure 12. FEM wall-pressure predictions for exercise 2: filling.

value, because full friction is not developed at every particle–wall contact. However, the global value of μ was very model dependent.

The continuum analyses could not represent the filling process at all, but had to take this as an *a priori* assumption. The filling height, initial density and angle of repose were all, therefore, set as initial conditions. Most discrete-element analyses did not produce a significant angle of repose, but some researchers argue that real hard circular rods give an experimental angle of repose close to zero (if so, circular rods are not very representative of real granular solids). An angle of repose comparable with the angle of internal friction is achievable by greatly increasing the rotational inertia of particles or by using non-circular particles (Potapov & Campbell 1998; Ting *et al.* 1993). The formulation of microscopic material parameters from known macroscopic material behaviour remains a major stumbling block for DEM in reliably modelling a real solid. A further major shortcoming of DEM is that accurate prediction of local stress states requires huge numbers of particles (not viable in most programs) because of the low signal–noise ratio in the data.

Much further research is needed on the prediction of the filling state in silos if DEM is to be a useful practical predictive tool. However, it seems likely that DEM will prove useful in explaining microscopic behaviours in solids, and will principally assist with the development of better macroscopic or continuum material models for use in other programs.

4. Discharge predictions

Two exercises on silo discharge were studied: discharge from a steep converging hopper and discharge from a silo with a flat base. These two exercises pose quite different challenges for numerical predictions: both are more difficult than the filling exercise. The results are fully documented in Sanad *et al.* (1997).

Discharge of a granular solid from a steep converging hopper results in mass flow (all particles are in motion). This is the simplest flow problem for continuum models.

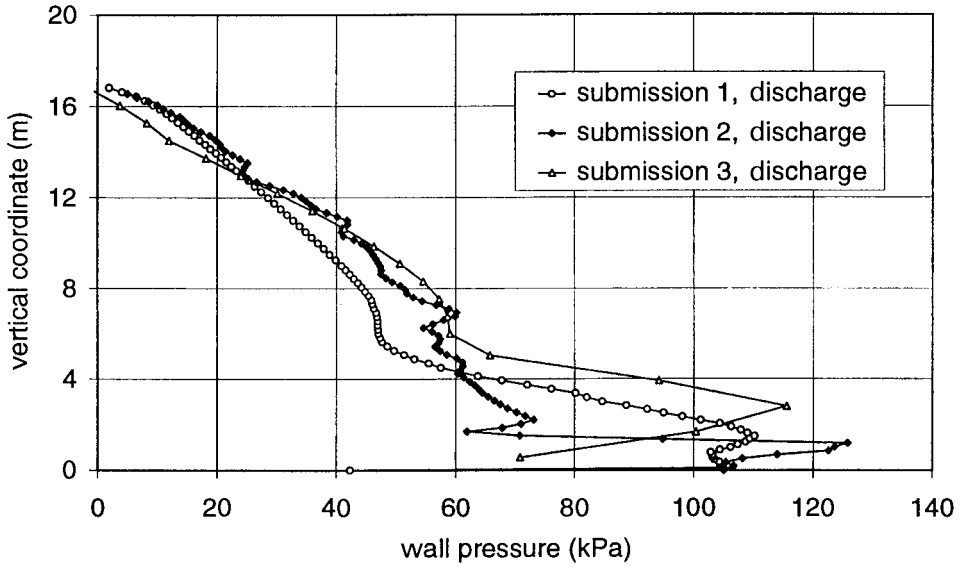

Figure 13. FEM wall-pressure predictions for exercise 2: discharge.

To ensure an effective challenge, the complete silo had a vertical parallel section above the hopper, giving a sharp transition junction. Discharge from a flat-bottomed silo results in internal flow with a stationary zone, which gives a flowing–static discontinuity at the boundary. This discontinuity presents a severe challenge to continuum models. Dilation, particle shape and packing structure often affect flow patterns strongly in experiments.

The problem description for these exercises was modified after analysis of the filling exercise, and care was taken to provide matching DEM and FEM descriptions of a single real material. The description was sent to some 130 groups: 25 submissions were received. Each submission contained the complete output after a filling step and at several instants during discharge: the total volume of data was huge.

The focus of the study was on the key elements of flow pattern, flow rate, wall-pressure pattern and local pressures at the transition, together with the other measures used for the filling problem. The expectations of the study were that pressure increases would occur early in the discharge, especially near the effective transition in the flat-bottomed silo, or the transition in the hopper silo, since these phenomena have often been observed experimentally.

(*a*) *Finite-element predictions*

The FEM calculations for both exercises provide a relatively homogeneous comparison: most of the calculations used a static analysis. In one of these (submission 3), the geometry of the flow channel boundary for exercise 2 was predefined. Only one submission (2) treated the discharge with a dynamic formulation.

After filling the flat-bottomed silo (exercise 2), three distinct wall-pressure patterns were observed (figure 12): submission 3 used progressive filling while the others did not. The program used for submission 2 has no corresponding calculation for exercise 1, and the curve may be noted as different in form.

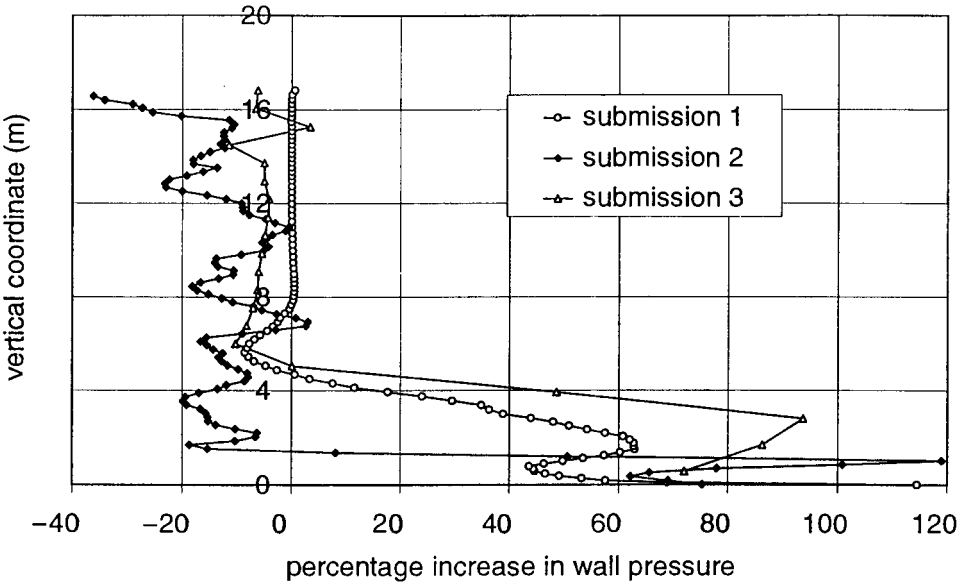

Figure 14. FEM wall-pressure predictions for exercise 2: increase from filling to discharge.

The discharge pressure distributions are shown in figure 13. All three show significant increases (figure 14) in the zone of static material below the effective transition (the point at which the flow-channel boundary meets the wall). Submissions 1 and 3 identify this point as *ca.* 5 m above the base, and show similar increases below it: submission 2 (dynamic analysis) places it much lower, perhaps too low to be credible for sand.

The changes in pressure from filling to discharge are always a focus of silo tests: figure 14 shows that submission 1 sees effectively no change in the upper part; submission 3 sees small reduction there; while submission 2 sees larger pressure reductions with rather erratic variations.

Two submissions were received for the hopper silo (exercise 3), both of which were static calculations from the same programs as for submissions 1 and 3 above. After filling, the two pressure distributions were similar (figure 15), and in the classic pattern for silos with hoppers (see, for example, Ooi & Rotter 1989) with a peak pressure at the transition. This peak is approximately 50% higher than the pressure value at mid-height inside the hopper. The pressure distributions in the vertical section are similar to those in the flat-bottomed silo. The discharge pressure pattern is shown in figure 16. The vertical section pressures are effectively unchanged, the hopper pressures are modified in form, and a local increase is seen in the peak pressure at the transition. However, only submission 1 indicates that this is a substantial rise. The patterns do not match classical hopper pressure theories (see, for example, Walters 1973*a*, *b*) very well.

The changes in pressure are shown in figure 17, which allows a clearer identification of the changes. In a real discharge, the pressure near the outlet should fall substantially on discharge: some doubt must be expressed about submission 3, therefore, since the pressure rises throughout the hopper.

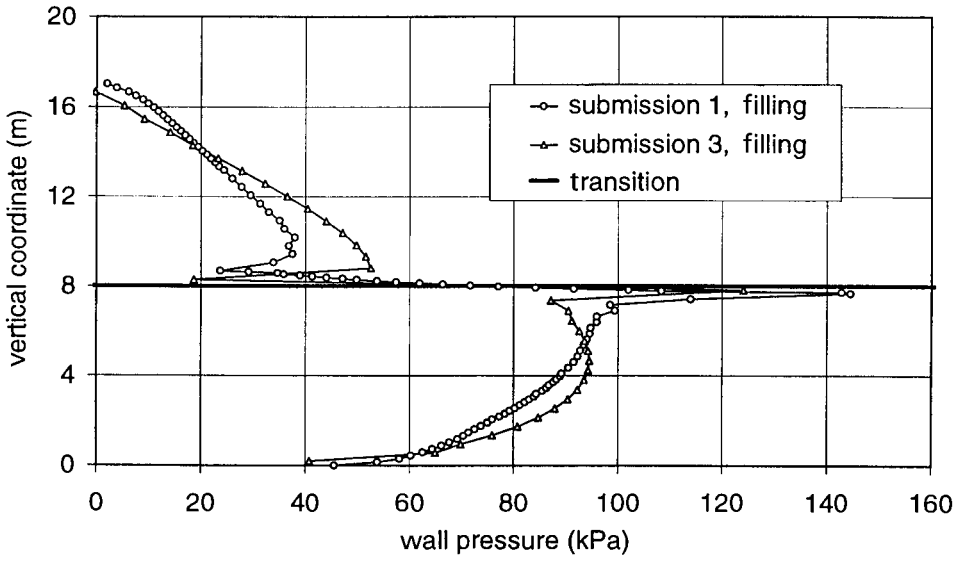

Figure 15. FEM wall-pressure predictions for exercise 3: filling.

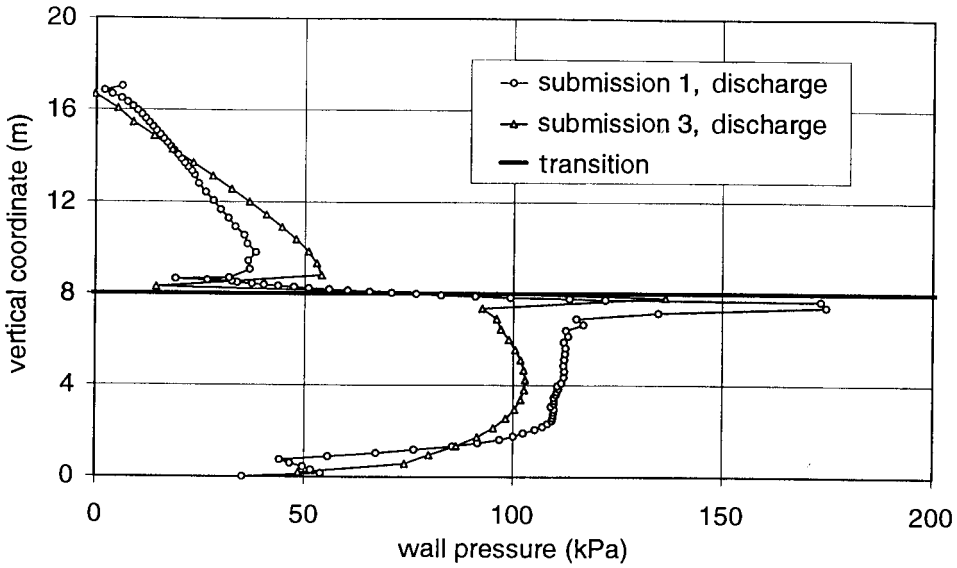

Figure 16. FEM wall-pressure predictions for exercise 3: discharge.

(*b*) *Discrete-element predictions*

(i) *Velocity fields*

An obvious advantage of DEM is its power to display velocity fields. These were plotted for all submissions to illustrate the onset of flow, the formation of a flow channel, localized flow patterns, the relative velocity of particles, and the discharge of solids from the silo. In the representations shown here for submission 1, velocities are plotted to scale for particles whose velocity exceeds 1 m s^{-1}. Other particles are

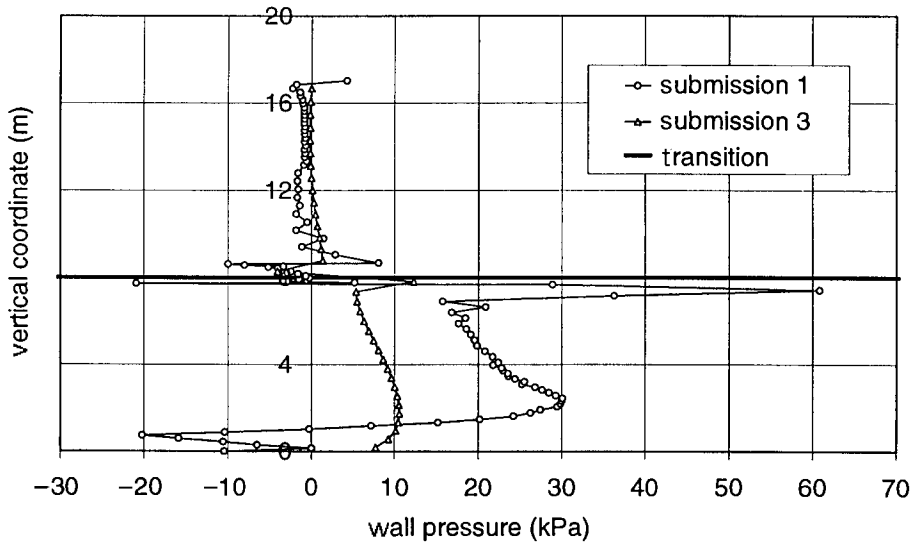

Figure 17. FEM wall-pressure predictions for exercise 3: increase from filling to discharge.

represented by points. This representation allows a rather clear distinction between the static and flowing zones in the bulk solid.

In the flat-bottomed silo of exercise 2 (figure 18), at the beginning of discharge (up to $t = 0.2$ s), only particles close to the outlet move (figure 18*a*). By 1 s, a flow pattern with a defined flow channel has been established (figure 18*b*) and the granular solid is effectively divided into a flowing zone and a dead zone. The flow-channel boundary reaches the wall at the 'effective transition', which is found at about $z = 8$ m. Above this point, almost all material is flowing. However, there are some local zones close to the wall where very small movements occur. Later in the discharge, velocity waves travel up the silo, so that the velocity at any point varies in an approximately cyclic manner: the top part of the bulk can be seen to have a lower velocity at $t = 8$ s (figure 18*c*): such waves are seen several times during the discharge.

In the hopper silo of exercise 3, propagation of a velocity 'wave' through the bulk solid can be seen clearly after the outlet is opened. Initially, only material close to the outlet flows (figure 19*a*), and the flow zone propagates upwards until the complete bulk solid is moving downwards by $t = 1$ s (figure 19*b*). This typical mass-flow pattern is retained to the end of the discharge (figure 19*c*). This pattern was seen in all submissions.

The flow phenomena seen in both discharge exercises were observed in almost all submissions and they appear to be relatively independent of the algorithms used in the models. Following much variation early in the discharge, the flow rate agreed quite closely between all submissions ($6.0\ \mathrm{m^3\ s^{-1}}\ \pm 5\%$), excluding calculations involving obvious blunders.

(ii) *Porosity*

The mean porosity of the bulk solid is a good global indicator of dilation in the material. It is plotted against time for all submissions for the flat-bottomed and

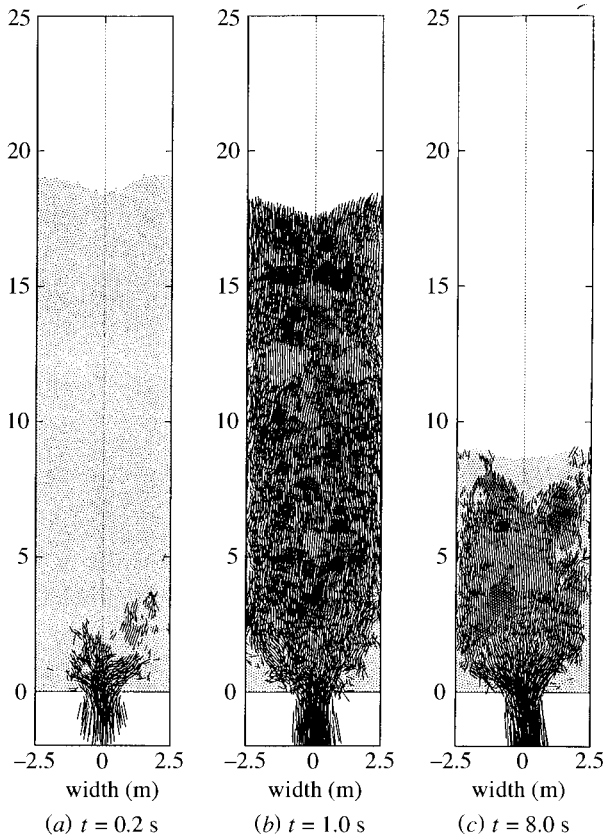

Figure 18. DEM velocity fields for exercise 2.

hopper silos in figure 20*a*, *b*, respectively. In all cases, the porosity increases over the first 0.5 s, corresponding to a local dilation near the outlet as flow commences.

After $t = 1$ s, the mean porosity remains rather constant for the flat-bottomed silo, but there is a progressive increase in porosity in the hopper silo. These phenomena were found in all submissions, despite significant differences of initial packing density.

(iii) *Angle of repose*

The average slope of the two sides of the top surface was determined as the 'angle of repose' at each time-step: a positive value indicates that the surface is convex.

In exercise 2 (flat-bottomed), the initial angle of repose varied widely between submissions (−15 to +31°). Negative values occurred in submissions 1, 2, 5 and 7 but positive values in submissions 3, 4 and 6. Most submissions predicted that the angle of repose is approximately constant for the first 2 s of discharge, followed by a reduction towards zero: this is understandable where the slope is positive, but puzzling when it is initially negative.

In exercise 3 (with hopper), the behaviour is similar, with an initial range of repose angles from −22 to +28°. Only two submissions had a convex top surface (4 and 6). One submission (3) had a highly convex surface in exercise 2, but a highly concave surface for exercise 3. The reasons for such effects are not clear.

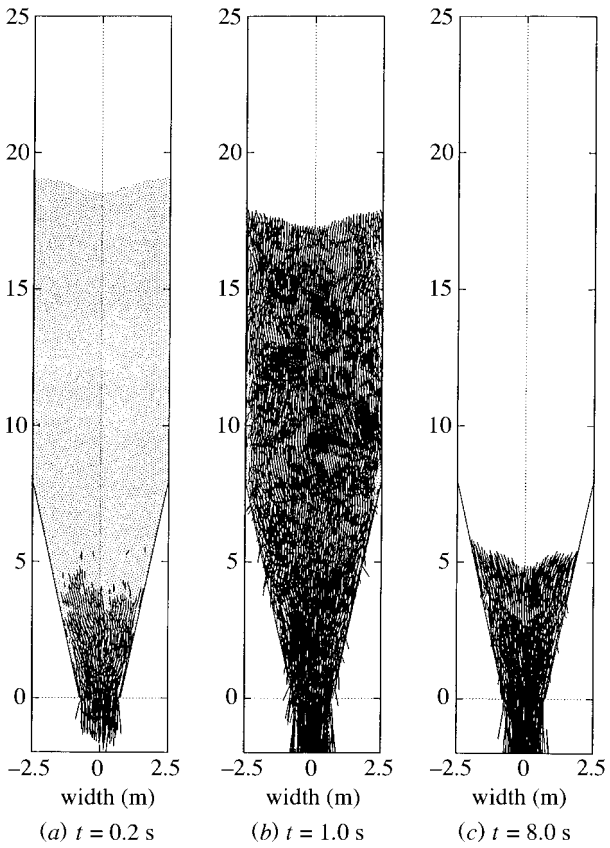

Figure 19. DEM velocity fields for exercise 3.

(iv) *Wall pressures*

The pressure distributions against the wall at each time-instant were found using a moving average over ten particles to produce smooth curves as before. After filling, a best-fit Janssen curve was again used to extract global properties. This also provided a reference curve for each calculation, against which the discharge predictions could be compared (as used in design standards).

While Janssen theory cannot be expected to represent pressures well during discharge, it still provided a useful means of comparison between filling and discharge. Attempts were made to extract parameters relating to other theories, such as switch-pressure interpretations (Walker 1964; Jenike *et al*. 1973; Walters 1973*a*), but without statistically significant success. For the silo with a conical hopper, the pressure distribution bore little relation to classical theories (Walker 1966; Walters 1973*b*), so only the wall pressures on the vertical walls were modelled with a best-fit Janssen curve.

The parameters obtained from the best-fit Janssen approximation of the filling data (Sanad *et al*. 1997) showed a similar wide range to that observed in exercise 1. In some calculations, there was a significant asymmetry, with the wall-pressure distribution differing considerably between the left and right walls. Figure 21 shows the mean of the left- and right-wall pressures up the silo for a typical example of a

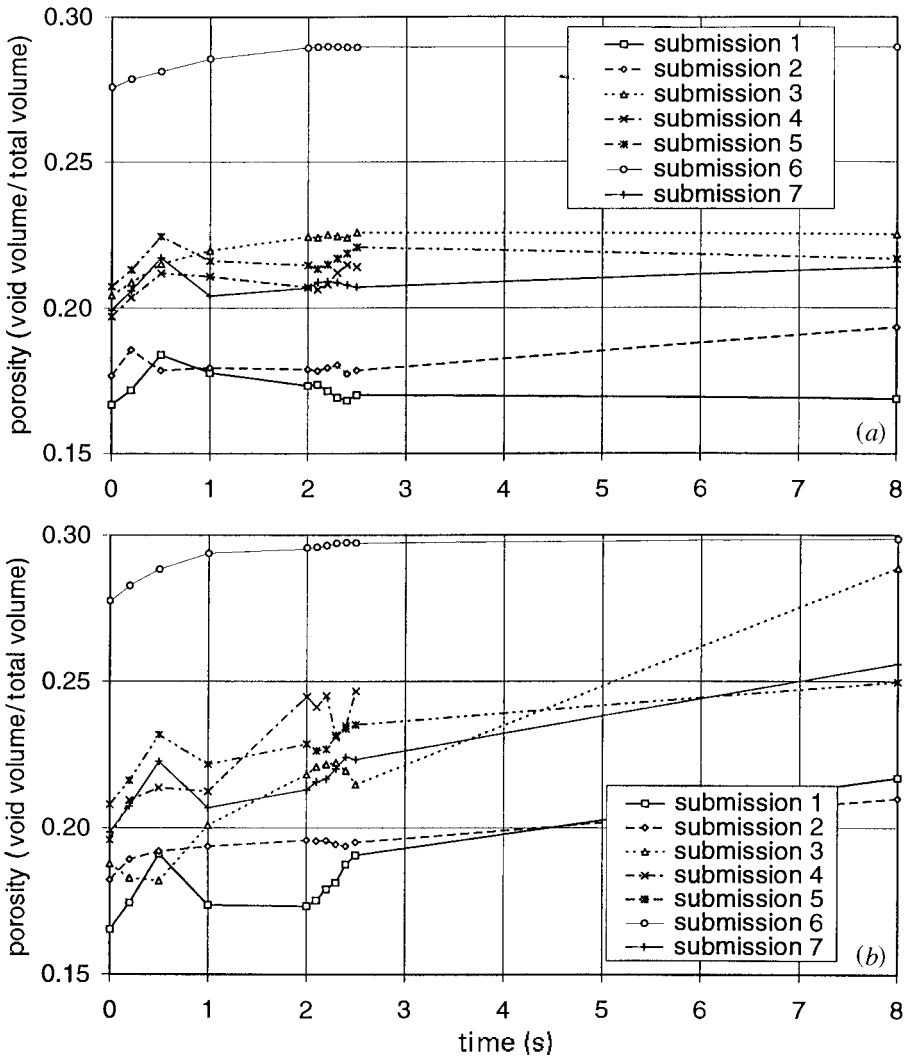

Figure 20. Mean porosity variations during discharge

flat-bottomed silo (exercise 2): the filling and discharge pressures are both shown. The Janssen best fit is also shown for each curve. The variation in pressures down the wall is clearly often great, but the mean pattern is clear.

When the best-fitting process was repeated for each instant during discharge, the Janssen parameters, k and μ, had changed only by small amounts, despite local large changes in pressure; the global wall-pressure distribution remained virtually unchanged from the filling state, allowing for the fall in the top surface. For silo-pressure studies, the interesting time is when the silo is essentially still full (to maximize pressures), but flow of the solids has been fully initiated. This was well represented here by the time $t = 1$ s.

In exercise 2 (flat-bottomed), the pressure peaks after 1 s of discharge were very localized, and most of the wall experienced a small fall in pressure (figure 21) asso-

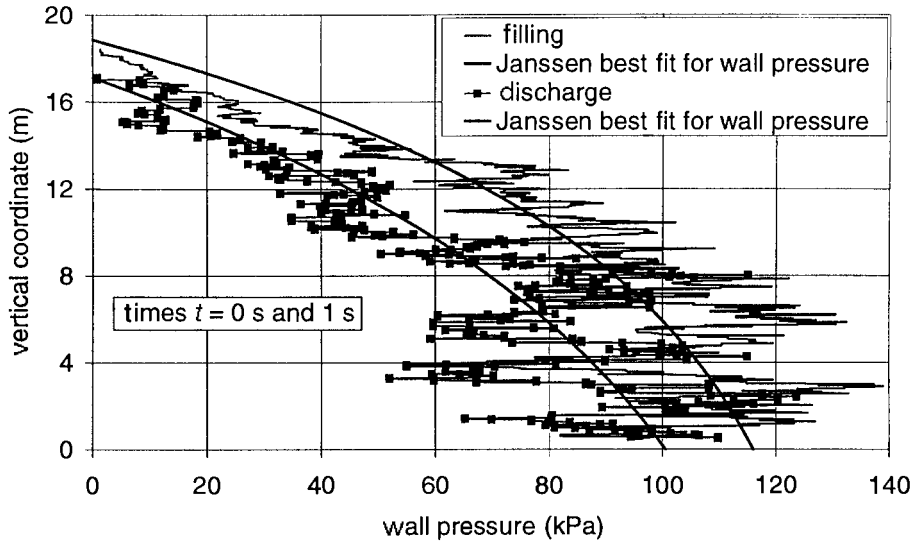

Figure 21. DEM wall-pressure predictions after filling and during discharge for exercise 2.

ciated with the falling upper surface (around 20%). It is possible that there is a focused peak-pressure region under discharge, between $z = 7$ m and $z = 9$ m, corresponding to the effective transition, but most local wall-pressure changes appear to occur randomly. This lack of a clear pattern of pressure change in figure 21 is found in all pressure variations at all instants and for all submissions received. Neither the location nor the value of local high pressures were common. Some calculations showed an overall increase in the mean pressure on the walls (a maximum of 21%), whereas others showed an overall decrease (a maximum of 35%).

The pressure distribution in exercise 3 (hopper silo) after filling is similarly non-uniform (figure 22). In loose terms, the pressures may seem to be slightly larger in the hopper than above the transition, but a clear pattern is difficult to discern. The pressures above the transition are quite well represented by the Janssen best-fit curve. The discharge pressures after 1 s are superposed on the filling values in figure 23 to illustrate the difficulty in making general statements. This submission shows a net increase in pressure in the hopper on discharge with very low pressures occurring near the outlet; this is a credible pattern, though it is hard to discern more detail. However, save for the low pressures near the outlet, the different submissions do not present a common picture. Both net increases and net decreases in the mean wall pressure are found during discharge.

(*c*) *Comparisons of discharge from a mass-flow converging hopper*

This exercise involves quite a complicated pattern of wall pressures with at least three separate zones: the vertical-walled section, the transition, and the hopper. The predictions must, thus, contain considerable refinement in local areas to predict both the form and magnitude of the pressures in each zone. Where high magnitude stochastic phenomena are superposed on the systematic forms, it may be difficult to deduce definitive patterns. The wall-pressure calculations from FEM are naturally much easier to assimilate than those from DEM. The DEM calculations could be

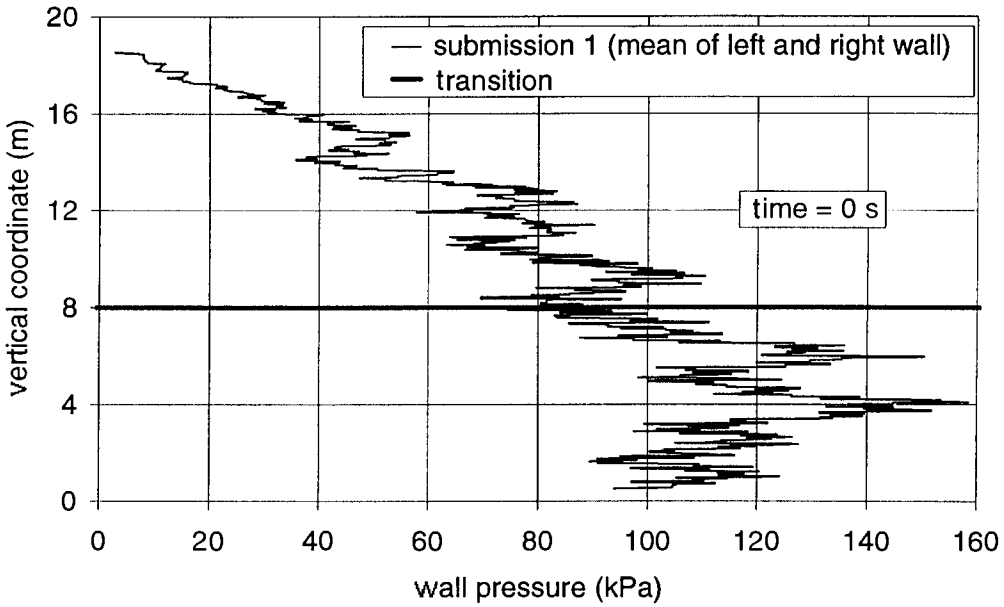

Figure 22. DEM wall-pressure predictions after filling for exercise 3.

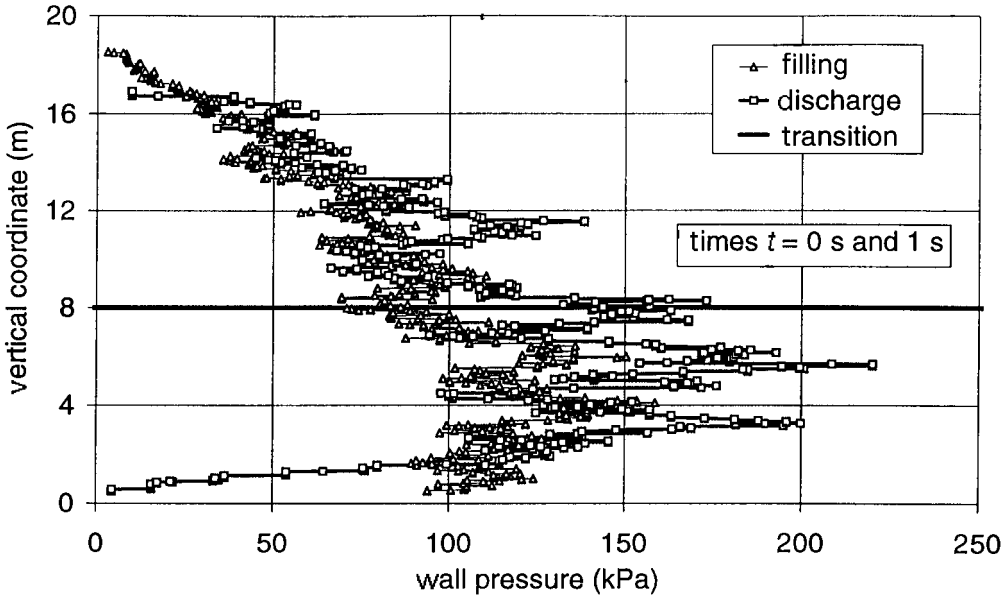

Figure 23. DEM wall-pressure predictions after filling and during discharge for exercise 3.

more revealing if a much larger number of particles could be used, permitting the scatter to diminish. The FEM analyses all produce very-high-pressure predictions at the transition junction, which may be in error and caused by the problem of defining the boundary condition there; DEM presents no such difficulty. Both types of analysis were able to show low pressures as the solid approaches the outlet. The flow rate is consistently well modelled by DEM.

(d) Comparisons of discharge from a flat-bottomed silo

This exercise involves an internal boundary between flowing and static solids. It was well defined in all DEM submissions with comparatively good agreement on its location. This suggests that the result is relatively model independent, though real experiments often show great sensitivity to packing structure (Nielsen 1998). However, measures of dilation or voidage in DEM showed a large variation between submissions. Most FEM calculations assumed the flow channel *a priori*. The form of the filling and discharge wall-pressure pattern was quite consistently predicted by FEM calculations, both quasi-static and dynamic, but the location of the effective transition was uncertain. Neither this pattern nor another competing one could be easily and consistently discerned in the DEM calculations. It is clear that complex patterns of pressure will only be obtainable from DEM calculations if very large numbers of particles are used. Pressure magnitudes in both DEM and FEM were consistent in order of magnitude, but rather scattered when any detail was examined.

5. General conclusions arising from the study

A very large difference was observed in the wall pressures estimated by FEM and DEM. This is mainly due to the different character of the two methods. The chief difficulty in comparing the two methods lies in the transformation of DEM individual particle forces into pressures to give a global mean pattern without loss of local systematic variations. The inherent scatter in DEM due to the microscopic behaviour of the solid tends to obscure global pressure patterns and means that very large numbers of particles are needed if DEM is to be used for quantitative silo calculations. Further research is needed to obtain results that can be compared between the two methods and even within each method.

DEM can give acceptable qualitative predictions of several dynamic phenomena that occur in silos, such as the development of flow patterns, arch formation and shear bands. In principle, it can also be used to follow the evolution of stresses in silos from the beginning of filling to the end of discharge. Although DEM is currently the most promising practical quantitative predictor of silo flow, it needs much further development before it can be used in engineering design.

By contrast, the FEM models can give credible quantitative predictions of silo pressures, but are currently unable to model the filling process, especially if the geometry and packing structure are to be determined. Most of the FEM models use simplifications, assume rather simple material behaviour, and do not properly deal with the dynamic discharge process. They also have difficulty with the boundary condition at the transition corner. Although FEM is currently the most promising practical quantitative predictor of silo pressures, it needs much further development before it can be used in engineering design.

The marked differences between the many submissions for these simple exercise problems from different leading research groups around the world indicate that much is still to be learned about the relationship between assumptions, constitutive models and computational algorithms and their resulting predictions. It is hoped that these exercise problems, so intensively studied already, will prove to be useful benchmarks for future program development.

The authors thank all those contributing to the project, all of whom should properly be named as co-authors and without whom the present study would have been impossible. A list of the

PHILOSOPHICAL TRANSACTIONS OF THE ROYAL SOCIETY A MATHEMATICAL, PHYSICAL & ENGINEERING SCIENCES

contributors is given in the appendix below. Many contributors provided considerable helpful advice as well as the requested calculations.

Financial support for this collaboration is gratefully acknowledged from the UK Engineering and Physical Sciences Research Council (EPSRC) under grant GR/J49631, and by the European Union under the BRITE/EURAM Concerted Action on Silos Research (CA-Silo) programme.

The encouragement, involvement and assistance with interpretation provided by Professor Juan Martinez of the Institut National des Sciences Appliquées de Rennes, France has been especially valuable.

Appendix A. Contributors

(*a*) *Continuum analysis*

1. P. Aguado, M. Guaita & F. Ayuga, Universidad Politecnica de Madrid, Spain.
2. M. El Yazidi & J. Martinez, INSA, Rennes, France.
3. L. A. Godoy & S. A. Elaskar, Universidad Nacional de Cordoba, Argentina.
4. T. Karlsson & M. Klisinski, Lulea University of Technology, Sweden.
5. L. Lehmann & H. Antes, Technische Universität Braunschweig, Germany.
6. M. Mehrafza & J. Eibl, Universität Karlsruhe, Germany.
7. I. D. Moore, University of Western Ontario, Canada.
8. J. M. Rotter, J. Y. Ooi, J. M. F. G. Holst & G. H. Rong, University of Edinburgh, UK.
9. A. M. Sanad, E. Ragneau & J. Aribert, INSA, Rennes, France.
10. J. P. J. Wittmer, University of Edinburgh, UK.
11. S. Xu & Q. Zhang, University of Manitoba, Canada.

(*b*) *Discrete-element analysis*

1. N. Bicanic, D. Owen & N. Petrinic, Universities of Glasgow and Swansea, UK.
2. M. Coetzee, D. Potyondy & P. A. Cundall, Itasca Consulting Group Inc., Minneapolis, USA.
3. C. Dury, Philipps-Universität, Marburg, Germany.
4. K. D. Kafui & C. Thornton, Aston University, Birmingham, UK.
5. N. Kruyt, University of Twente, The Netherlands.
6. M. Kuhn, University of Portland, Oregon, USA.
7. P. Langston & U. Tüzün, University of Surrey, Guildford, UK.
8. Z. Lu, J. Jofriet & S. Negi, University of Guelph, Oregon, Canada.
9. J. Martinez, INSA, Rennes, France.
10. G. Mischel & J. Ting, University of Massachusetts, Lowell, USA.

11. Y. Muguruma & Y. Tsuji, Osaka University, Japan.
12. A. Potapov & C. Campbell, University of Southern California, Los Angeles, USA.
13. G. Ristow, Philipps-Universität, Marburg, Germany.
14. G. H. Rong, J. M. Rotter, J. Y. Ooi, J. M. F. G. Holst & A. M. Sanad, University of Edinburgh, UK.
15. H. Sakaguchi, Kobe University, Japan.
16. S. Schrans & R. Daling, Koninklijke Shell-Laboratorium, Amsterdam, The Netherlands.
17. C. Wassgren, A. Karion, M. Hunt & C. Brennen, California Institute of Technology, USA.

References

ABAQUS 1997 *ABAQUS theory manual*, version 5.7. Pawtucket, RI: Hibbit, Karlsson & Sorensen Inc.

Aribert, J. M. & Ragneau, E. 1990 Stress calculations in silos by finite element method using different behaviour laws for the ensiled material. In *10th Int. Congr. of Chem. Engng, Chem. Equipment Design and Automation, Prague, Czechoslovakia, Aug. 1990*. European Federation of Chemical Engineers.

Askari, A. H. & Elwi, A. E. 1988 Numerical prediction of hopper-bin pressures. *J. Engng Mech. ASCE* **114**, 342–352.

Bishara, A. G., Mahmoud, M. H. & Chandrangsu, K. 1977 Finite element formulation for farm silo analysis. *J. Struct. Div. ASCE* **103**, 1903–1919.

Bishara, A. G., El-Azazy, S. S. & Huang, T. D. 1981 Practical analysis of cylindrical farm silos based on finite element analysis. *ACI Jl* **78**, 456–462.

Boyce, J. R. 1980 A non-linear model for the elastic behaviour of granular materials under repeated loading. In *Soils under cyclic and transient loading*, pp. 285–294. Rotterdam: Balkema.

Eibl, J. & Rombach, G. 1988 Numerical investigations on discharging silos. In *ICONMIG, Innsbruck, Austria, April 1988*.

Eibl, J., Landahl, H., Häußler, U. & Gladen, W. 1982 Zur frage des silodrucks. *Beton- und Stahlbetonbau* **77**, 104–110.

Häußler, U. & Eibl, J. 1984 Numerical investigations on discharging silos. *J. Engng Mech. ASCE* **110**, 957–971.

Holst, J. M. F. G., Rotter, J. M., Ooi, J. Y. & Rong, G. H. (eds) 1997 Discrete particle and continuum modelling of particulate solids in silos: silo filling. Report no. R97-007, Department of Civil and Environmental Engineering, University of Edinburgh.

Holst, J. M. F. G., Rotter, J. M., Ooi, J. Y. & Rong, G. H. 1999*a* Numerical modelling of silo filling. Part 1. Problem description and finite element analyses. *J. Engng Mech. ASCE*. (In the press.)

Holst, J. M. F. G., Rotter, J. M., Ooi, J. Y. & Rong, G. H. 1999*b* Numerical modelling of silo filling. Part 2. Discrete element analyses and comparisons. *J. Engng Mech. ASCE*. (In the press.)

Janbu, N. 1963 Soil compressibility as determined by oedometer and triaxial tests. In *Proc. European Conf. on Soil Mech. and Foundation Engng* **1**, pp. 19–25.

Janssen, H. A. 1895 Versuche über getreidedruck in silozellen. *Z. Vereines Deutscher Ingenieure* **39**, 1045–1049.

Jenike, A. W., Johanson, J. R. & Carson, J. W. 1973 Bin loads. Parts 2–4. *J. Engng for Industry, Trans. ASME* B **95**,1–5, 6–12, 13–16.

Jofriet, J. C., LeLievre, B. & Fwa, T. F. 1977 Friction model for finite element analyses of silos. *Trans. ASAE* C **2**, 735–744.

Kafui, K. D. & Thornton, C. 1995 Some aspects of silo discharge: computer simulations. In *Proc. Third European Symp. Storage and Flow of Particulate Solids (Janssen Centennial), Nuremberg, Germany, 21–23 March*, pp. 379–388. Nuremberg: Nuremberg Messe GmbH.

Karlsson, P., Klisinski, M. & Runesson, K. 1998 Finite element simulations of granular material flow in plane silos with complicated geometry. *Powder Technol.* **99**, 29–39.

Lade, P. 1977 Elastic-plastic stress strain theory for cohesionless soils with curved yield surfaces. *Int. J. Solids Struct.* **13**, 1019–1035.

Langston, P. A., Heyes, D. M. & Tüzün, U. 1994 Continuous potential discrete particle simulations of stress and velocity fields in hoppers. *Chem. Engng Sci.* **49**, 1259–1275.

Langston, P. A., Heyes, D. M. & Tüzün, U. 1995 Discrete element simulation of granular solid flow in hoppers: discharge rate and wall stress predictions in 2 & 3 dimensions. *Chem. Engng Sci.* **50**, 967–980.

Mahmoud, A. A. & Abdel-Sayed, G. 1981 Loading on shallow cylindrical flexible grain bins. *J. Powder Bulk Solids Tech.* **5**, 12–19.

Ooi, J. Y. & Rotter, J. M. 1989 Elastic and plastic predictions of the storing pressures in conical hoppers. *Trans. Mech. Engng IEAust.* **ME14**, 165–169.

Ooi, J. Y. & Rotter, J. M. 1990 Wall pressures in squat steel silos from finite element analysis. *Comp. Struct.* **37**, 361–374.

Potapov, A. V. & Campbell, C. S. 1998 A fast model for the simulation of non-round particles. *Granular Matter* **1**, 9–14.

Ragneau, E., Aribert, J. M. & Sanad, A. M. 1994 Modélisation numérique par élément fini tridimensionnel pour le calcul des actions aux parois des silos (remplissage et vidange). *Construction Métallique* **2**, 3–25.

Rotter, J. M., Pham, L. & Nielsen, J. 1986 On the specification of loads for the structural design of bins and silos. In *Proc. 2nd Int. Conf. on Bulk Materials Storage Handling and Transportation, July*, pp. 241–247. Wollongong, Australia: IEAust.

Rotter, J. M. & Ooi, J. Y. 1995 Problem definition for filling of a silo. Comparative evaluation of numerical methods for predicting flow and stress fields in silos. Report on EPSRC DEM/FEM International Collaboration, Department of Civil and Environmental Engineering, University of Edinburgh.

Rotter, J. M., Ooi, J. Y., Rong, G. H. & Holst, J. M. F. G. 1996 Problem definition for discharging of a silo. Comparative evaluation of numerical methods for predicting flow and stress fields in silos. Report on EPSRC DEM/FEM International Collaboration, Department of Civil and Environmental Engineering, University of Edinburgh.

Runesson, K. & Nilsson, L. 1986 Finite element modelling of the gravitational flow of a granular material. *Bulk Solids Handling* **6**, 877–884.

Sakaguchi, E., Kawakami, S. & Tobita, F. 1996 Simulation on flowing phenomena of grains by distinct element method. Report no. 94-G-25, Tokyo University of Agriculture.

Sakaguchi, H. & Ozaki, E. 1993 Analysis of the formation of arches plugging the flow of granular materials. In *Powders and grains 1993* (ed. C. Thornton). Rotterdam: Balkema.

Sanad, A. M., Holst, J. M. F. G., Ooi, J. Y. & Rotter, J. M. (eds) 1997 Discrete particle and continuum modelling of particulate solids in silos: silo discharge. Report R97-011, Department of Civil and Environmental Engineering, University of Edinburgh.

Savage, S. B. 1992 Some aspects of confined granular flows. In *Tagungsberichte Silos—Forschung und Praxis, Karlsruhe, Germany, October*, pp. 111–120. Universität Karlsruhe, Germany.

Schmidt, L. C. & Wu, Y. H. 1989 Prediction of dynamic wall pressures on silos. *Bulk Solids Handling* **9**, 333–338.

Smith, D. L. O. & Lohnes, R. A. 1982 Frictional properties and stress–strain relationships for use in finite element analysis of grain silos. *J. Powder Bulk Solids Tech.* **6**, 4–10.

Tejchman, J. & Gudehus, G. 1993 Silo-music and silo-quake: experiments and numerical Cosserat approach. *Powder Technol.* **76**, 201–212.

Thornton, C. 1991 Computer simulated hopper flow. In *4th World Congr. of Chem. Engng: STRATEGIES 2000, Karlsruhe, Germany, 16–21 June*. European Federation of Chemical Engineers.

Ting, J. M., Khwaja, M., Meachum, L. R. & Rowell, J. D. 1993 An ellipse-based discrete element model for granular materials. *Int. J. Numer. Analysis Meth. Geomech.* **17**, 603–623.

Walker, D. M. 1964 A theory of gravity flow of cohesive powders. R&D Dept Report no. 22, Central Electricity Generating Board, South West Region, UK.

Walker, D. M. 1966 An approximate theory for pressure and arching in hoppers. *Chem. Engng Sci.* **21**, 975–997.

Walters, J. K. 1973*a* A theoretical analysis of stresses in silos with vertical walls. *Chem. Engng Sci.* **28**, 13–21.

Walters, J. K. 1973*b* A theoretical analysis of stresses in axially-symmetric hoppers and bunkers. *Chem. Engng Sci.* **28**, 779–789.

Wieckowski, Z. & Klisinski, M. 1995 Finite deformation analysis of motion of granular material in silo. *Arch. Mech.* **47**, 617–633.

Wu, Y. H. & Schmidt, L. C. 1992 Comparison of calculated and observed filling and flow pressures in silos and hoppers. In *Proc. 4th Int. Conf. on Bulk Solids Storage Handling and Transportation, July*, pp. 449–452. Wollongong, Australia: IEAust.

Yagi, J., Akiyama, T. & Hogami, H. 1995 Simulation of solid flow in moving beds. In *Proc. 3rd European Symp. Storage and Flow of Particulate Solids (Janssen Centennial), Nuremberg, Germany, 21–23 March*, pp. 347–356. Nuremberg: Nuremberg Messe GmbH.

PHILOSOPHICAL TRANSACTIONS OF THE ROYAL SOCIETY A MATHEMATICAL, PHYSICAL & ENGINEERING SCIENCES